2016 14th International Conference on Control, Automation, Robotics & Vision
Phuket, Thailand, 13-15th November 2016 (ICARCV 2016)

Image-based Visual Tracking Adaptive Control for Mobile Robots

Ying Zou, Changyun Wen, Mao Shan, Mingyang Guan
School of Electrical and Electronic Engineering
Nanyang Technological University
Singapore (639798)
Email: zouy0011@e.ntu.edu.sg; ecywen@ntu.edu.sg; shanmao@ntu.edu.sg; myguan@ntu.edu.sg

***Abstract*—In this paper, we deal with the problem of image-based visual tracking for mobile robots. It is noted that the presence of actuator dynamics and the unknown target motion increases the complexity of the system model and makes the design of the controller more difficult. To solve this problem, we propose an adaptive control approach via utilizing backstepping technique and extended state observer (ESO). For the controller design, the adaptive technique is employed to estimate the bound of the target motion and the adaptive law is derived from the Lyapunov stability theory. We also adopt two ESOs to estimate and compensate for the disturbances affecting the mobile robot dynamics and the wheel actuator dynamics. It is shown that the proposed adaptive controller guarantees the boundness of all the signals in the closed-loop system and enables the tracking errors to exponentially converge to a compact set which is adjustable.**

I. Introduction

During the past few decades, image-based visual tracking control for mobile robots has received extensive attention. It has been addressed by researchers for a wide range of applications including surveillance, inspection, and automatic mobile robot navigation [1]-[2]. In many applications, mobile robots need to track moving objects with the aid of visual feedback from cameras mounted on them. Technically, image-based visual tracking deals with the problem of locking the projection of the target object on the image plane to a particular position by controlling robot motion. Therefore, a visual tracking controller based on the sensed positions of the target object is required for the mobile robot. For an image-based visual tracking system, the control design involves constructing system model and developing control method.

In terms of system model, firstly, a camera-target visual interaction model is required to develop the map between the image plane velocities and the velocities of the camera and the target in the world frame [3]. However, most existing visual interaction models, see for examples [4]-[5], neglect the motion of the target in the 3D space. Meanwhile, the model of a robot is another important component of the system model. So far, many robot models have been developed to realize velocity control or torque control for mobile robot [2], [6]-[7]. Note that the wheels of a mobile robot are driven by actuators. However, the dynamics of the actuators are excluded from the modelling in these works. In fact it has been shown in [8] that the dynamics of actuators should be taken into consideration to ensure a reliable and meaningful control performance.

On the basis of system model and visual feedback, research efforts have been contributed to tracking control for mobile robots. Based on backstepping idea, a visual feedback controller is used to control a mobile robot to track a moving target in [7]. However, the proposed controller cannot maintain the control performance when the velocities of the target are unknown. To address the influence of target motion, a visual state estimator (VSE) based on Kalman filter is introduced to estimate the target motion in [9]. However, the conditions of implementing Kalman filter such as Gaussian distribution of uncertainty, smoothness motion and uniform sampling rate, are quite strong and thus still restrict the performance of the proposed VSE.

Motivated by the aforementioned researches, we address the image-based visual tracking control for a mobile robot equipped with an on-board camera in this paper. The target motion, robot dynamics and wheel actuator dynamics are all taken into account in the system model. Furthermore, the target motion is unknown, and there are unknown bounded disturbances affecting the robot dynamics and the wheel actuator dynamics. To solve this problem, an adaptive controller is developed by using backstepping technique and ESOs. Our main approaches and contributions compared to existing results in this area are summarized as follows.

1) The wheel actuator input voltages are chosen as the control inputs, which is more realistic than most of existing controllers where torques and velocities are chosen as the inputs, respectively.

2) The target motion is taken into account, which has been neglected or assumed to be known in many of the existing methods.

3) Based on backstepping technique, adaptive control scheme and linear ESOs are employed to estimate and compensate for the unknown target motion and the unknown disturbances, respectively.

4) The proposed control method is analysed to establish that all the signals in the closed-loop system are uniformly ultimately bounded and the tracking error converges to a compact set which is adjustable.

The remaining part of the paper is organized as follows. The system models including the visual interaction model, robot dynamics and wheel actuator dynamics are described

978-1-5090-3549-6/16/$31.00

in Section II. Section III presents the methods of designing and analyzing the adaptive controller. Simulation results are presented in Section IV, and conclusions are given in Section V.

II. System model

Considering a mobile robot tracking system as shown in Fig. 1. Suppose that a camera is mounted along the heading direction of the mobile robot with its optical centre P_0 at the centre of the wheel axis. A coordinate frame R_p is attached to the optical centre P_0 , with its y-axis and the z-axis orthogonal to the motion plane and along the optical axis of the camera, respectively, as shown in Fig. 2 where the perspective projection model of the camera is given. The image plane π is perpendicular to the optical axis and lies at a distance λ from the optical centre, with its axes parallel to x and y axes of R_p.

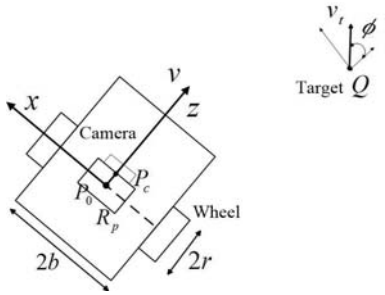

Fig. 1. Top view of the configuration of a mobile robot

A. Camera motion and the interaction matrix

The position of the target with respect to R_p is defined as $Q = (X, Y, Z)$. Let q be the projection of Q on the image plane. The vector $s = [x, y]^T$ thus gives the image coordinates of q on the image plane. Using the pin-hole model for the camera (shown in Fig. 2), we obtain the following relationships:

$$\frac{X}{x} = \frac{Y}{y} = \frac{Z}{\lambda} \tag{1}$$

where Z can be obtained by the camera.

Let ν_t and ϕ be the linear velocity of the target object Q and the angle between the target heading direction and the z-axis of R_p. Since the camera is fixed to the robot, then both the camera and the mobile robot have the same linear and angular velocity, respectively denoted as ν and ω. Then the motion of the target with respect to the camera can be given as follows [7]:

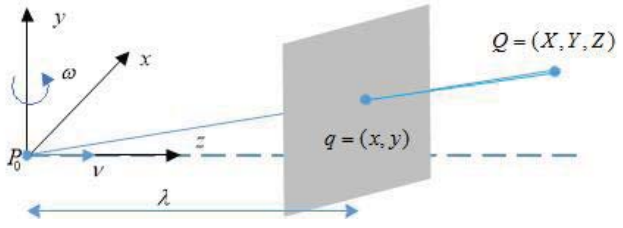

Fig. 2. Coordinate systems relationship

$$\begin{bmatrix} \dot{X} \\ \dot{Z} \end{bmatrix} = \begin{bmatrix} \nu_t \sin\phi - Z\omega \\ -\nu + \nu_t \cos\phi + X\omega \end{bmatrix} \tag{2}$$

Substituting (2) into (1), the visual interaction mapping between velocities in the image plane and the world frame can be established as follows

$$\begin{aligned} \dot{s} &= \begin{bmatrix} -\frac{x}{yZ} & \frac{\lambda}{Z} \\ -\frac{y}{Z} & 0 \end{bmatrix} \begin{bmatrix} \nu_t \cos\phi \\ \nu_t \sin\phi \end{bmatrix} + \begin{bmatrix} -\frac{x}{Z} & -\frac{\lambda^2+x^2}{\lambda} \\ \frac{y}{Z} & -\frac{xy}{\lambda} \end{bmatrix} \begin{bmatrix} \nu \\ \omega \end{bmatrix} \\ &= \Phi\theta + T\eta \end{aligned} \tag{3}$$

where $\theta = \begin{bmatrix} \nu_t \cos\phi & \nu_t \sin\phi \end{bmatrix}^T$, T is the interaction matrix and $\eta = [\nu \quad \omega]^T$.

B. Kinematic and dynamic of the mobile robot

Based on the assumption that the mobile robot moves on a 2-D plane without slips, the relationship between the robot velocities and the wheels angular velocities can be given as [10],

$$\eta = \overline{J}\varpi \tag{4}$$

where $\varpi = [\omega_1 \quad \omega_2]^T$ denotes the angular velocities of the left and right wheels of the mobile robot,

$$\overline{J} = \frac{r}{2} \begin{bmatrix} 1 & 1 \\ b^{-1} & -b^{-1} \end{bmatrix} \tag{5}$$

b and r are the half width of the mobile robot and the radius of the wheel.

Then the dynamics of the mobile robot in terms of ϖ can be written as

$$\overline{M}\dot{\varpi} + \overline{C}(\eta)\varpi + \overline{\varepsilon} = \tau \tag{6}$$

where $\overline{M}$ is a symmetric, positive definite inertia matrix, $\overline{C}$ is the centripetal and Coriolis matrix, $\overline{\varepsilon}$ is a vector of external time-varying disturbances, $\tau = [\tau_1 \quad \tau_2]^T$ represents the control torques applied to the wheels. The expressions of matrices $\overline{M}$ and $\overline{C}$ are the same as those in [10].

Using (4), the visual interaction model (3) can be rewritten as

$$\dot{s} = \Phi\theta + J\varpi \tag{7}$$

where $J = T\overline{J}$. The dynamic equation (6) can also be rewritten as follows,

$$\dot{\varpi} = -C(\eta)\varpi + B\tau + \varepsilon \tag{8}$$

where $C(\eta) = \overline{M}^{-1}\overline{C}(\eta)$, $B = \overline{M}^{-1}$ and $\varepsilon = [\varepsilon_1 \quad \varepsilon_2]^T = -B\overline{\varepsilon}$.

C. Wheels actuator dynamics

The wheels of the robot are driven by actuators which are assumed to be DC motors with mechanical gears. It is necessary to take the dynamics of such motors into account.

$$L_m\dot{I}_m + R_m I_m + K_e\omega_m + \overline{d} = u \tag{9}$$

$$\tau_m = K_t I_m, \tau = N\tau_m, \omega_m = N\varpi \tag{10}$$

where L_m, R_m, K_e and K_t are positive definite constant diagonal matrices denoting inductance, resistance, back electromotive force constant and torque sensitivity of the motors,

respectively. u, I_m, τ_m and ω_m are the input voltages, current, the output torques and angular velocities of the motors, respectively. $\bar{d}$ represents unknown voltage disturbances. N is the gear ratio.

Then the dynamics of the motors can be described as

$$\dot{\tau} = -R\tau - K_1\varpi + K_2 u + d \tag{11}$$

where $R = L_m^{-1}R_m$, $K_1 = L_m^{-1}N^2K_tK_e$, $K_2 = L_m^{-1}NK_t$ and $d = (d_1, d_2)^T = -K_2\bar{d}$.

By using (7), (8) and (11), the system model of the mobile robot including the camera projection, robot kinematics, robot dynamics and wheel actuator dynamics can be summarized as

$$\dot{s} = \Phi\theta + J\varpi \tag{12}$$

$$\dot{\varpi} = -C(\eta)\varpi + B\tau + \varepsilon \tag{13}$$

$$\dot{\tau} = -R\tau - K_1\varpi + K_2 u + d \tag{14}$$

The control objective is to find an image-based tracking control scheme applied to the mobile robot to ensure the target object staying at the desired position of the image plane. More specifically, we will design an adaptive controller for the input voltage u such that the projection of the target Q on the image plane, q, asymptotically approaches the desired position while all the signals in the system are bounded.To achieve this control objective, we need the following assumptions

Assumption. 1 *The unknown target motion term θ is bounded, namely, there exists $\nu_t \cos\phi < \delta_1$ and $\nu_t \sin\phi < \delta_2$ where δ_1 and δ_2 are positive constants.*

Assumption. 2 *The unknown disturbances ε and d and their first-order derivatives are bounded.*

Remark. 1 *The successful experiments in [11] and [12] indicate that the Assumption.2 is feasible and reasonable in real applications.*

To realize a good control performance, we will compensate for the effects of target motion and disturbances by designing an online parameter estimator to estimate the unknown bounds $\delta = [\delta_1, \delta_2]^T$ and two ESOs to estimate ε and d.

III. Controller design

To realize the control objective mentioned in Section II, a new controller design approach is proposed in this section. Our idea is to employ backstepping technique to design an auxiliary wheel angular velocity controller, an auxiliary torque controller and an actuator voltage controller to make the tracking error as small as possible. Furthermore, an online parameter estimator and two ESOs are designed to estimate and compensate for the unknown target motion and disturbances, respectively.

Step. 1 *Design of the auxiliary controller for ϖ*

For the sake of tracking objective, define the image-based tracking error as

$$e_1 = s - s_d \tag{15}$$

where $s_d = \begin{bmatrix} x_d & z_d \end{bmatrix}^T$ is the desired position on the image plane. Then the derivative of e_1 is given by

$$\dot{e}_1 = \dot{s} - \dot{s}_d = \Phi\theta + J\varpi \tag{16}$$

The auxiliary controller for ϖ is chosen as

$$\varpi_d = -J^{-1}\Gamma_1 e_1 + J^{-1}g_1 \tag{17}$$

where Γ_1 is a positive definite constant matrix and and g_1 is a component used to compensate for θ.

In real application, since the target motion is unknown, θ and its bound are all unknown. To compensate for the effect of the target motion, a real time estimator is employed to estimate the bound of θ. Then g_1 in the auxiliary controller ϖ_d (17) and the estimator can be designed as

$$g_1 = -\Phi sgn(e_1^T\Phi) * \hat{\delta} \tag{18}$$

$$\dot{\hat{\delta}} = W^{-1}\left|\Phi^T e_1\right| \tag{19}$$

where $sgn(e_1^T\Phi) * \hat{\delta} = [sgn(e_1^T\Phi_1)\hat{\delta}_1, sgn(e_1^T\Phi_2)\hat{\delta}_2]^T$ with $\hat{\delta} = [\hat{\delta}_1, \hat{\delta}_2]^T$ being the estimation of δ and $\Phi_i, i = 1, 2$ representing the ith column of Φ, W is a positive definite constant matrix. The estimation error of δ is defined as

$$\tilde{\delta} = \delta - \hat{\delta} \tag{20}$$

Substituting the auxiliary controller (17) and (18) into (16) results in the error dynamic

$$\dot{e}_1 = -\Gamma_1 e_1 + Je_2 + \Phi\theta - \Phi sgn(e_1^T\Phi) * \hat{\delta} \tag{21}$$

where $e_2 = \varpi - \varpi_d$.

Step. 2 *Design of the auxiliary controller for τ*

Based on (13), the auxiliary controller for τ is chosen as

$$\tau_d = B^{-1}(\dot{\varpi}_d + C(\eta)\varpi - \Gamma_2 e_2 - J^T e_1 + g_2) \tag{22}$$

where Γ_2 is a positive definite constant matrix, g_2 is a component used to compensate for ε.

Substituting the auxiliary controll (22) into (13) results in the error dynamics

$$\dot{e}_2 = -\Gamma_2 e_2 - J^T e_1 + Be_3 + g_2 + \varepsilon \tag{23}$$

where $e_3 = \tau - \tau_d$.

Since ε is unknown and cannot be obtained exactly by the measurements of sensors, an ESO is employed to estimate and compensate for ε. Extend ε as an additional state variable by defining $x_1 = e_2$ and $x_2 = \varepsilon$ and let $h_1(t)$ represent the variation rate of ε. Then the original error dynamic model in (23) is now described as

$$\begin{aligned} \dot{x}_1 &= f_1 + g_2 + x_2 \\ \dot{x}_2 &= h_1(t) \end{aligned} \tag{24}$$

where $f_2 = -\Gamma_2 x_1 - J^T e_1 + Be_3$.

Then an ESO can be constructed as follows

$$\begin{aligned} \dot{\hat{x}}_1 &= f_1 + g_2 + \hat{x}_2 - 2\rho_1(\hat{x}_1 - x_1) \\ \dot{\hat{x}}_2 &= -\rho_1^2(\hat{x}_1 - x_1) \end{aligned} \tag{25}$$

where $\rho_1 > 0$ is the desired pole of the ESO, $\hat{x}_1$ and $\hat{x}_2$ are the estimations of e_2 and ε.

The detailed analysis of ESO can be seen in [12] and [13]. Define $\tilde{x}_i = x_i - \hat{x}_i$, $i = 1, 2$ as the estimation errors of the ESO.

Lemma. 1 [13] : *Since $h_1(t)$ is bounded from Assumption.2, then the estimated states and estimation errors are always bounded and there exists a constant $\delta_{1i} > 0$ and a finite time $T_1 > 0$ such that*

$$\|\tilde{x}_i\| \leq \xi_{1i}, \quad \xi_{1i} = \mathrm{O}(\frac{1}{\rho_1^j}); \qquad i = 1, 2, \quad \forall t \geq T_1 \tag{26}$$

for some positive integer j.

Remark. 2 *The results of Lemma.1 indicate that the introduced ESO has an excellent steady observation performance. After a finite time, the estimation errors can be compressed to a prescribed range which can be arbitrarily small by increasing the design parameter ρ_1.*

Therefore, based on the estimated state $\hat{x}_2$, g_2 can be designed as follows,

$$g_2 = -\hat{x}_2 + g_{2s} \tag{27}$$

where g_{2s} is a control function which satisfies the following condition,

$$e_2^T[g_{2s} + \tilde{x}_2] \leq \sigma\xi_{12}^2 \tag{28}$$

An example of g_{2s} satisfying (28) is given by

$$g_{2s} = -\frac{e_2}{4\sigma} \tag{29}$$

where σ is a positive design parameter.

Substituting (27) and (29) into (23) results in the state error dynamics

$$\dot{e}_2 = -\Gamma_2 e_2 - J^T e_1 + Be_3 + \tilde{x}_2 - \frac{e_2}{4\sigma} \tag{30}$$

Step. 3 *Design of the controller for u*

After the torque controller τ_d being designed, the wheel actuator voltage controller u is chosen as

$$u = K_2^{-1}(\dot{\tau}_d - \Gamma_3 e_3 - B^T e_2 + R\tau + K_1\varpi + g_3) \tag{31}$$

where Γ_3 is a positive definite constant matrix, g_3 is a component used to compensate for d.

Substituting the controller (31) into (14) results in

$$\dot{e}_3 = -\Gamma_3 e_3 - B^T e_2 + d + g_3 \tag{32}$$

To handle the unknown disturbance d, an ESO can also be employed to estimate d by defining $z_1 = e_3$, $z_2 = d$ and letting $h_2(t)$ represent the variation rate of d. Then the error dynamic model (32) is rewritten as

$$\begin{aligned} \dot{z}_1 &= f_2 + g_3 + z_2 \\ \dot{z}_2 &= h_2(t) \end{aligned} \tag{33}$$

where $f_2 = -\Gamma_3 e_3 - B^T e_2$.

Now an ESO is constructed for the dynamic model (33) as follows

$$\begin{aligned} \dot{\hat{z}}_1 &= f_2 + g_3 + \hat{z}_2 - 2\rho_2(\hat{z}_1 - z_1) \\ \dot{\hat{z}}_2 &= -\rho_2^2(\hat{z}_1 - z_1) \end{aligned} \tag{34}$$

where $\rho_2 > 0$ is the desired pole of the ESO, $\hat{z}_1$ and $\hat{z}_2$ are the estimations of e_3 and d. The estimation errors of the ESO are defined as

$$\tilde{z}_i = z_i - \hat{z}_i, i = 1, 2 \tag{35}$$

Lemma. 2 [13] : *Since $h_2(t)$ is bounded, then the estimated states and estimation errors are always bounded and there exists a constant $\eta_{2i} > 0$ and a finite time $T_2 > 0$ such that*

$$\|\tilde{z}_i\| \leq \xi_{2i}, \quad \xi_{2i} = \mathrm{O}(\frac{1}{\rho_2^k}); \qquad i = 1, 2, \quad \forall t \geq T_2 \tag{36}$$

for some positive integer k.

Based on the estimated state $\hat{z}_2$, g_3 is designed as

$$g_3 = -\hat{z}_2 - \frac{e_3}{4\sigma} \tag{37}$$

Substituting (37) into (32) results in

$$\dot{e}_3 = -\Gamma_3 e_3 - B^T e_2 + \tilde{z}_2 - \frac{e_3}{4\sigma} \tag{38}$$

Now we can summarize the designed adaptive controller as follows:

$$\varpi_d = -J^{-1}(\Gamma_1 e_1 + \Phi sgn(e_1^T\Phi) * \hat{\delta}) \tag{39}$$

$$\tau_d = B^{-1}(\dot{\varpi}_d + C(\eta)\varpi - \Gamma_2 e_2 - J^T e_1 - \hat{x}_2 - \frac{e_2}{4\sigma}) \tag{40}$$

$$u = K_2^{-1}(\dot{\tau}_d - \Gamma_2 e_3 - B^T e_2 + R\tau + K_1\varpi - \hat{z}_2 - \frac{e_3}{4\sigma}) \tag{41}$$

with the update law (19) and two ESOs in (25) and (34).

Theorem. 1 *For the system modelled by* (12), (13) *and* (14), *the controller consisting of* (19), (25), (34) *and* (39)-(41) *guarantees that all the signals in the closed-loop system are bounded and after a finite time $T_m = \max(T_1, T_2)$ where T_1 and T_2 are respectively given in Lemmas 1 and 2, the tracking errors exponentially converge towards a compact set which is adjustable.*

Proof.

Consider the following Lyapunov candidate function

$$V = \frac{1}{2}(e_1^T e_1 + \tilde{\delta}^T W\tilde{\delta} + e_2^T e_2 + e_3^T e_3) \tag{42}$$

Differentiating V with respect to time and using the error dynamics (21), (30) and (38), yields

$$\begin{aligned}\dot{V} &= e_1^T\dot{e}_1 + \tilde{\delta}^T W\dot{\tilde{\delta}} + e_2^T\dot{e}_2 + e_3^T\dot{e}_3 \\ &= e_1^T(-\Gamma_1 e_1 + Je_2 + \Phi\theta - \Phi\mathrm{sgn}(e_1^T\Phi) * \hat{\delta}) - \tilde{\delta}^T\left|\Phi^T e_1\right| \\ &+ e_2^T(-\Gamma_2 e_2 - J^T e_1 + Be_3 + \tilde{x}_2 - \frac{e_2}{4\sigma}) \\ &+ e_3^T(-\Gamma_3 e_3 - B^T e_2 + \tilde{z}_2 - \frac{e_3}{4\sigma}) \\ &= -e_1^T\Gamma_1 e_1 - e_2^T\Gamma_2 e_2 - e_3^T\Gamma_3 e_3 + e_1^T\Phi\theta \\ &- e_1^T\Phi\mathrm{sgn}(e_1^T\Phi) * \hat{\delta} - \tilde{\delta}^T\left|\Phi^T e_1\right| + e_2^T\tilde{x}_2 - \frac{e_2^T e_2}{4\sigma} \\ &+ e_3^T\tilde{z}_2 - \frac{e_3^T e_3}{4\sigma} \\ &\leq -e^T\Gamma e + \left|e_1^T\Phi\right|\delta - \left|e_1^T\Phi\right|\hat{\delta} - \tilde{\delta}^T\left|\Phi^T e_1\right| \\ &+ e_2^T\tilde{x}_2 - \frac{e_2^T e_2}{4\sigma} + e_3^T\tilde{z}_2 - \frac{e_3^T e_3}{4\sigma} \\ &\leq -e^T\Gamma e + + e_2^T\tilde{x}_2 - \frac{e_2^T e_2}{4\sigma} + e_3^T\tilde{z}_2 - \frac{e_3^T e_3}{4\sigma}\end{aligned} \tag{43}$$

where $\Gamma = diag\{\Gamma_1, \Gamma_2, \Gamma_3\}$, $e = \left[e_1^T, e_2^T, e_3^T\right]^T$.

The target motion, the disturbances and the variation rates of disturbances are assumed to be bounded. For $t < T_m$, from Lemma.1 and Lemma.2, we know that all the estimation errors are always bounded. From (43), it is easy to know that all the signals are bounded for $t < T_m$.

Furthermore, for $t > T_m$, from Lemma.1 and Lemma.2 we have

$$\dot{V} \leq -e^T\Gamma e + \|e_2\|\xi_{12} - \frac{\|e_2\|^2}{4\sigma} + \|e_3\|\xi_{22} - \frac{\|e_3\|^2}{4\sigma} \tag{44}$$

Define $\lambda_{\min}$ as the minimum eigenvalue of matrix Γ. It is easy to know that

$$e^T e = 2V - \beta \tag{45}$$

where $\beta = \tilde{\delta}^T W\tilde{\delta}$, and it is easy to know that $\beta \geq 0$.

Substituting (45) into (44) and noting (28), yields in the following inequality

$$\dot{V} \leq -\zeta V + \mu \tag{46}$$

where $\zeta = 2 * \lambda_{\min}$ and $\mu = \beta\lambda_{\min} + \sigma(\xi_{12}^2 + \xi_{22}^2)$.

From (46) we have

$$\frac{1}{2}\sum_{i=1}^{3} e_i \leq V \leq e^{-\zeta(t-T_m)}V(T_m) + \frac{\mu}{\zeta}(1 - e^{-\zeta(t-T_m)}) \tag{47}$$

So V is bounded, thus $e_i, i = 1, 2, 3$ is bounded by a function that conveges exponentially towards a compact set $\Omega = \left\{e \middle| \|e\|^2 \leq 2\frac{\mu}{\zeta}\right\}$ at a rate of ζ. The size of Ω can be reduced by decreasing σ or increasing $\lambda_{\min}(\Gamma)$.

IV. Simulations

In this section, a simulation example will be provided to show the effectiveness of the proposed control method. The sampling period is 0.01s. The parameters of the robot dynamic model are given as follows:

$$\bar{M} = \begin{bmatrix} 0.0746 & -0.0296 \\ -0.0296 & 0.0746 \end{bmatrix}$$

,

$$\bar{C} = \begin{bmatrix} 0 & 1.125 \times 10^{-3}(\omega_1 - \omega_2) \\ -1.125 \times 10^{-3}(\omega_1 - \omega_2) & 0 \end{bmatrix}$$

The paraeters of the wheel acuators are chosen as $R = diag(135.25, 135.25)$, $K_1 = diag(30.942, 30.942)$ and $K_2 = diag(85.95, 85.95)$. The target velocity term in the interaction model and the disturbances affecting the mobile robot dynamics and the wheel actuator dynamics are set as $\theta = \begin{bmatrix} 0.5\sin(t + \pi/5) \\ 0.5\cos(t + \pi/6) \end{bmatrix}$, $\bar{\varepsilon} = \begin{bmatrix} 2.6\cos(3.3t + \pi/7) + e^{-t} \\ 2\cos(2.7t + \pi/3) + 1.2e^{-t} \end{bmatrix}$ and $\bar{d} = \begin{bmatrix} 1.3\sin(2.35t - \pi/6) + 1.45\cos(1.75t + \pi/9) \\ 1.3\sin(3.17t) + 1.4\cos(1.85t + \pi/7) \end{bmatrix}$, respectively.

The physical parameters of the camera are set as: focal length $\lambda = 35mm$ and resolution is 512×512 pixels (x and y were scaled to pixels for visualization purposes). The size of the image is 512×512 pixels. The initial position and the desired position of the target on the image plane are $s = \begin{bmatrix} -200 & 200 \end{bmatrix}^T$ and $s_d = \begin{bmatrix} 0 & 10 \end{bmatrix}^T$, respectively. The desired poles of the ESOs are $\rho_1 = \rho_2 = 45$, positive definite constant matrices $\Gamma_1 = \Gamma_2 = \Gamma_3 = diag(4, 4)$ and $\sigma = 0.3$.

To validate the effectiveness of the proposed method, a comparison between the controller based on the proposed method and a controller designed using the standard backstepping approach without any consideration of the target motion and disturbances is carried out. The parameters of the standard backstepping approach are the same as those of the proposed control method. Fig.3 and Fig.4 show the motion trajectories of the projection of the target on the image plane. In Fig.5, the tracking errors are illustrated.

Due to the unknown target motion and disturbances, it is difficult for the standard backstepping control to achieve a satisfactory control performance. The maximum tracking errors in steady state are 49.01 pixels on $x-$axis and 2.32 pixels on $y-$pixels, respectively. On the other hand, owing to the online parameter estimator and the ESOs that are employed to estimate and compensate for the target motion and disturbances, the proposed control method gives a better control performance with the maximum tracking errors in steady state are 2.08 pixels on $x-$axis and 0.1 pixels on $y-$axis, respectively. Such enhancement of control performance indicates the effectiveness of the parameters estimator and ESOs.

V. Conclusion

The design of image-based visual tracking control for mobile robots is not a simple task. First, the target motion in the visual interaction model is unknown when the target is moving during operation. Second, since the wheels of the robot are driven by the motors, the resulting system should be represented as a third-order dynamic model.

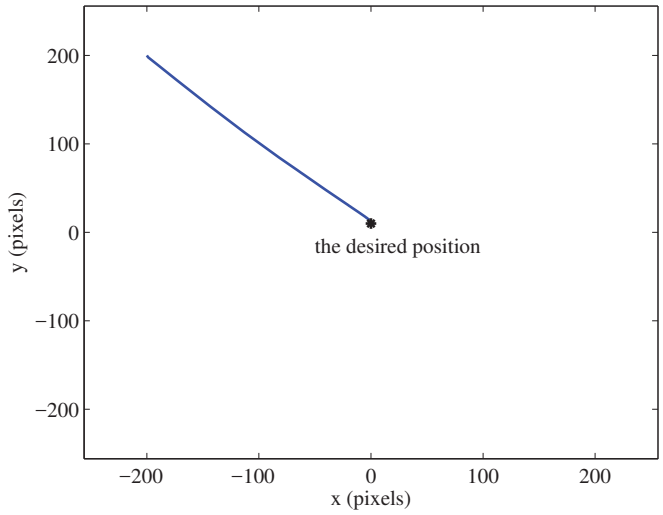

Fig. 3. The trajectory of projection on the image plane by using the proposed control method

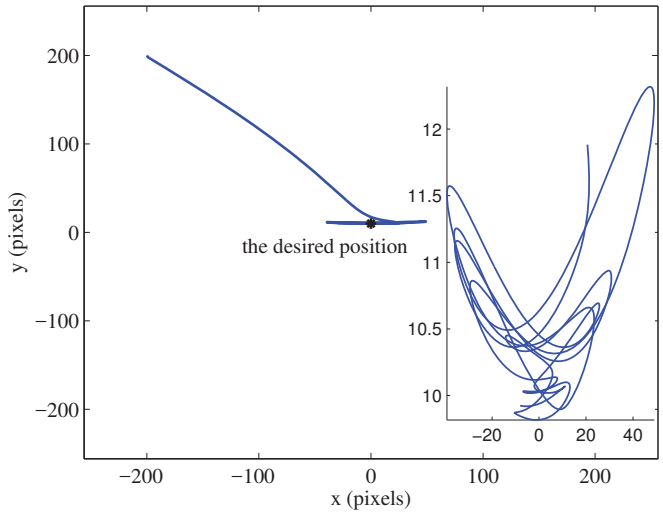

Fig. 4. The trajectory of projection on the image plane by using the standard backstepping approach

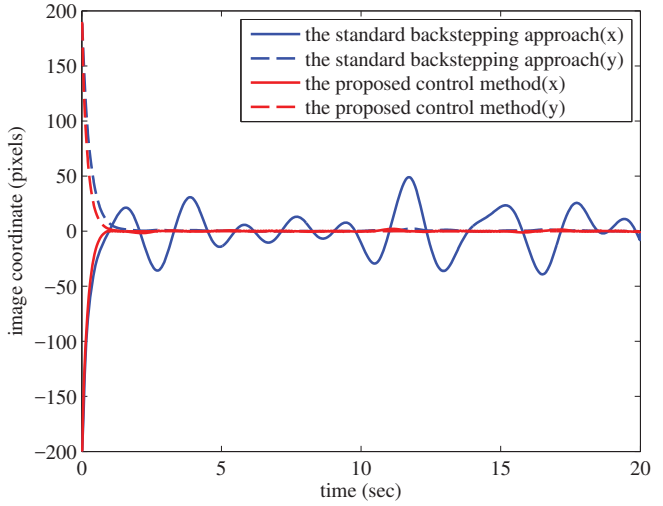

Fig. 5. The tracking errors with the two control methods

To address these problems, we firstly develop a system model taking the target motion and the wheel actuator dynamics into account, then design an adaptive controller by using the backstepping technique and ESO. An online parameter estimator is employed to estimate the bound of the target motion. Furthermore, the disturbances affecting the mobile robot dynamics and wheel actuator dynamics are estimated and compensated by two linear ESOs. Both theoretical analysis and simulations are provided to prove and illustrate the feasibility of the proposed approach.

REFERENCES

[1] L. Weiss, A. Sanderson, and C. Neuman, "Dynamic sensor-based control of robots with visual feedback," *IEEE Journal on Robotics and Automation*, vol. 3, no. 5, pp. 404–417, 1987.

[2] J. Jean, F. Lian, Z. Chen, and C. Jiao, "Robust visual servo control of a mobile robot for object tracking using shape parameters," *IEEE Transactions on Control Systems Technology*, vol. 20, no. 6, pp. 1461–1472, 2012.

[3] P. Corke and S. Hutchinson, "A new partitioned approach to image-based visual servo control," *IEEE Transactions on Robotics and Automation*, vol. 17, no. 4, pp. 507–515, 2001.

[4] M. W. Spong, S. Hutchinson, and M. Vidyasagar, "Robot modeling and control. 2006."

[5] B. Tamadazte, N. Le-Fort Piat, and E. Marchand, "A direct visual servoing scheme for automatic nanopositioning," *Mechatronics, IEEE/ASME Transactions on*, vol. 17, no. 4, pp. 728–736, 2012.

[6] C. Lazar and A. Burlacu, "A control predictive framework for image-based visual servoing applications," in *Advances in Robot Design and Intelligent Control*, 2016, pp. 185–193.

[7] H. Wang, S. Itani, T. Fukao, and N. Adachi, "Image-based visual adaptive tracking control of nonholonomic mobile robots," in *Intelligent Robots and Systems, 2001. Proceedings. 2001 IEEE/RSJ International Conference on*, vol. 1, 2001, pp. 1–6.

[8] T. Das and I. N. Kar, "Design and implementation of an adaptive fuzzy logic-based controller for wheeled mobile robots," *Control Systems Technology, IEEE Transactions on*, vol. 14, no. 3, pp. 501–510, 2006.

[9] C.-Y. Tsai, K.-T. Song, X. Dutoit, H. Van Brussel, and M. Nuttin, "Robust visual tracking control system of a mobile robot based on a dual-jacobian visual interaction model," *Robotics and Autonomous Systems*, vol. 57, no. 6, pp. 652–664, 2009.

[10] J. Huang, C. Wen, W. Wang, and Z.-P. Jiang, "Adaptive stabilization and tracking control of a nonholonomic mobile robot with input saturation and disturbance," *Systems & Control Letters*, vol. 62, no. 3, pp. 234–241, 2013.

[11] Z.-H. Wang and Z.-H. Liu, "Application of active disturbance rejection controller in wheeled mobile robot servo system," in *Guidance, Navigation and Control Conference (CGNCC), 2014 IEEE Chinese*, 2014, pp. 324–329.

[12] J. Yao, Z. Jiao, and D. Ma, "Adaptive robust control of dc motors with extended state observer," *Industrial Electronics, IEEE Transactions on*, vol. 61, no. 7, pp. 3630–3637, 2014.

[13] Q. Zheng, L. Gao, and Z. Gao, "On stability analysis of active disturbance rejection control for nonlinear time-varying plants with unknown dynamics," in *Proceedings of the IEEE Conference on Decision and Control, New Orleans, LA, Dec*, pp. 12–14.